Minimum time reference trajectory generation for an autonomous quadrotor

Elie Kahale, Pedro Castillo Garcia, Yasmina Bestaoui

Minimum Time Reference Trajectory Generation for an Autonomous Quadrotor

E. Kahale, P. Castillo and Y. Bestaoui

Abstract— **A three dimension trajectory generation and tracking for an autonomous quadrotor is studied in this paper. The vehicle is represented as one point which is its center of gravity, and only the kinematic equations are considered for trajectory generation problem. The model is derived using Newton's second law. The proposed trajectory generation method allows the computation of a time optimal trajectory which satisfies vehicle's capacity and minimizes traveled time between an initial configuration and a final one. Next, the obtained reference trajectory is applied to the full quadrotor dynamic model and an autopilot to ensure the trajectory tracking is designed. Numerical simulations with different scenarios are realized in order to illustrate the proposed trajectory generation method and validate the designed tracking strategy.**

I. Introduction

Unmanned **A**erial **V**ehicles (**UAV**s) have gained, in the last two decades, enough of technological maturity and user acceptance to move from revolutionary concept to evolutionary development. They are now desired in many nations because of their many advantages such as inexpensiveness, ease of maintenance, the multiplicity of their applications, and the most important, the protection of human pilots from risks [1]. The ability of rotor-crafts to take off and land in limited spaces and to hover above targets, gives such kind of UAVs the superiority over fixed wing aircrafts for surveillance and inspection missions. Since the quadrotor is mechanically simpler and easier to operate and repair than a conventional helicopter, this type of aerial vehicle is privileged.

The crucial elements to ensure the autonomy of UAVs are trajectory generation and tracking. This paper deals with these two aspects. First of all, we focus on the problem of calculating reference trajectories. These trajectories must minimize the traveled time and meet the physical constraints of the aerial vehicle. After that, we design an autopilot to track the obtained trajectory and evaluate its compatibility with the dynamics of quadrotor.

The problem of minimum time trajectory is equivalent to minimum path length problem proposed by Dubins in [2]. He proved the existence of shortest path between two specified points for a vehicle moving in a 2D plan with a constant velocity. In addition, he showed that the optimal paths are a combination of three segments at most. These portions take the form of circular arcs and straight lines. Based on Dubins results, the authors in [3] - [5] have proposed algorithms to generate a feasible paths taking into account kinematic and tactical constraints imposed on the UAV. A dynamic trajectory smoothing algorithm on horizontal plan was presented in [6]. Their idea is to smooth path segments in order to obtain an extremal trajectory with explicit consideration of kinematic constraints. A generalization of the previous method is shown in [7], where a 3D trajectory planner based on initial trim elementary trajectories was suggested. Similarly, another solutions based on splines are proposed to compute feasible trajectories in [8]-[11].

The trajectory generation algorithm proposed in this work is based on the optimality notion. Thus, it minimizes the arrival time to the desired point and takes the physical constraints of the vehicle into account. These restrictions can be regarded as limitations on flight path angle, velocity and their rate of change respectively as well as the rate of change of heading angle. Likewise in this work, we are interested in a quadrotor dedicated for inspection missions, which requires the presence of a camera attached to the vehicle. This camera, is supposed to be fixed in a specified position corresponding to the longitudinal axis of the vehicles. Hence, two scenarios for simulations have been taken. The first one deals with an aerial vehicle moving at a constant altitude. While, the second one treats the three dimensions trajectory generation problem. The obtained results, for both schemes, incorporate trajectory with multi-waypoints for a structure inspection task. The originality of our work is twofold : Firstly, adopting a point mass model to generate reference trajectories for a quad-rotor craft. Secondly, generalizing Dubins planning approach to 3D space planning and taking into account the advantage of the variation of the vehicle's velocity.

The paper is organized as follows : in section II, the quadrotor equations of motion are introduced. Time optimal trajectory generation problem is addressed in section III. In addition, the tracking problem is described in section IV. Some simulations are carried out to evaluate the proposed methods and are shown in section IV. Finally, conclusions are discussed in section VI.

II. Equations of motion

In this work, the quadrotor is modeled in two different manners. In the first one, the vehicle is presented as a rigid body evolving in the space due to the main thrust and three torques. This model is used in the trajectory tracking problem. Moreover on the second one, the aircraft is presented as one point which is its center of gravity. This representation is used for trajectory generation.

E. Kahale and Y. Bestaoui are with the IBISC EA 4526, Université d'Evry Val d'Essonne, France (e-mail: (kahale,bestaoui)@iup.univ-evry.fr)

P. Castillo is with LAFMIA laboratory, UMI 3275, CINVESTAV - IPN, Mexico (e-mail: castillo@hds.utc.fr).

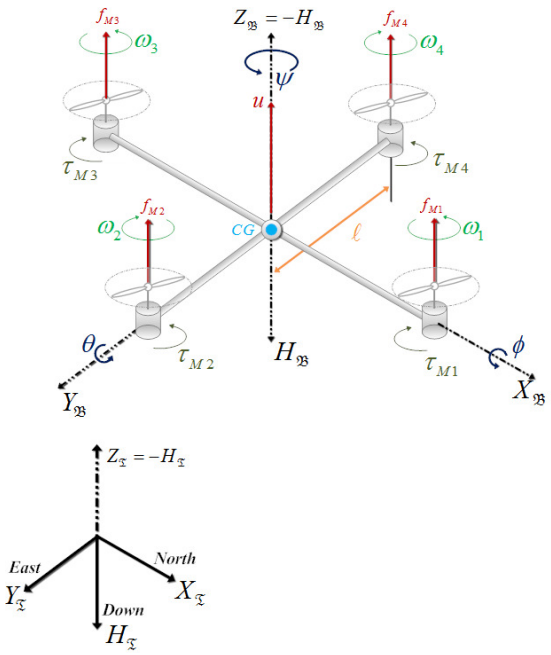

Fig. 1. The model of quad-rotor.

A. Rigid Body Model

The quadrotor is an underactuated system because it has four inputs and six degrees of freedom. It is controlled by varying the speeds of its four motors. Each one produces a thrust f_{Mi}, and the sum of these thrusts generate the main thrust of the vehicle $u = \sum_{i=1}^{4} f_{Mi}$. The difference in the rotor blade speed between the front motor and the rear one produces the pitch torque $\tau_\theta = (f_{M1} - f_{M3})\,\ell$. The roll torque is produced in a similar way $\tau_\phi = (f_{M2} - f_{M4})\,\ell$, and the yaw torque is the sum of the torques of each motor $\tau_\psi = \sum_{i=1}^{4} \tau_M$, see Figure 1. Notice that the front and the rear motors rotate counterclockwise, while the other two motors rotate clockwise. In addition, by its configuration and arrangement of the rotors, the gyroscopic effects and the aerodynamic torques tend to cancel in quasi-stationary maneuvers.

Remark that the roll angle must be near zero for mission requirements. Thus, we assume the existence of an automatic pilot which ensures the stabilization of ϕ close to zero.

Therefore, the generalized coordinates of the rotorcraft are

$$\varphi = (\zeta, \eta) \in \mathbb{R}^6 \tag{1}$$

where $\zeta = (x, y, z) \in \mathbb{R}^3$ denotes the position of the center of gravity of the vehicle relative to a fixed inertial frame $\mathcal{I}$, and $\eta = (\psi, \theta, \phi) \in \mathbb{R}^3$ presents the orientation of the vehicle expressed in the Euler angles (ψ for yaw, θ for pitch and ϕ for roll).

Then, the simplified nonlinear quadrotor mathematical representation is given by the following equations

$$m\ddot{x} = -u \sin\theta \tag{2a}$$
$$m\ddot{y} = u \cos\theta \sin\phi \tag{2b}$$
$$m\ddot{z} = u \cos\theta - mg \tag{2c}$$
$$\ddot{\psi} = \tau_\psi \tag{2d}$$
$$\ddot{\theta} = \tau_\theta \tag{2e}$$
$$\ddot{\phi} = \tau_\phi \tag{2f}$$

For more details see [12].

B. Point Mass Model

A configuration q_i of quadrotor at a specified time t_i is a vector defining the position $\zeta(t_i)$, the orientation $\eta(t_i)$, and velocity $V(t_i)$ of the aerial vehicle. Thus, let us define

$$q_i = (\zeta(t_i), \eta(t_i), V(t_i)) \in \mathbb{R}^6 \tag{3}$$

In order to reach a specified (final) configuration q_f from the actual (initial) one q_0, it follows from equations (2) and (3) that the time profile of x, y, z, θ, ψ, V, $\dot{\theta}$, $\dot{\psi}$, and $\dot{V}$ must be known along all the trajectory. Hence, from trajectory generation point of view, the quad-rotor can be presented by its center of gravity (CG). This model is known as Point Mass Model and is resulted from Newton's second laws of motion. It describes the relative velocity vector $\overrightarrow{V}$ with respect to an inertial frame and the external forces acting on the vehicle. In addition, this model is mathematically accurate under the assumption of flat earth and symmetric flight case ; the last supposition means that the sideslip angle is zero [15].

The states of the model are down-range x, cross-range y, altitude z, flight path angle γ, heading angle χ, and velocity V. By definition, the flight path angle γ is the angle between $\overrightarrow{V}$ and its projection in the $x \times y$ plane. On the other hand, the pitch angle is given as the sum of the flight path angle and the angle of attack [18]

$$\theta = \gamma + \alpha \tag{4}$$

For quadrotor vehicle the angle of attack is very small and consequently it can be neglected ($\alpha \approx 0$). Thus, equation (4) becomes

$$\theta = \gamma \tag{5}$$

Besides, the heading angle χ is measured from the north to the projection of $\overrightarrow{V}$ in the local horizontal plane. Then, it can be regarded as the yaw angle ψ. Thus,

$$\chi = \psi \tag{6}$$

From the previous discussion and from Figure 2, we can state

$$\dot{\overrightarrow{r}} = \overrightarrow{V} \tag{7}$$

Consequently we obtain,

$$\dot{x} = V \cos\psi \cos\theta \tag{8a}$$
$$\dot{y} = V \sin\psi \cos\theta \tag{8b}$$
$$\dot{z} = V \sin\theta \tag{8c}$$

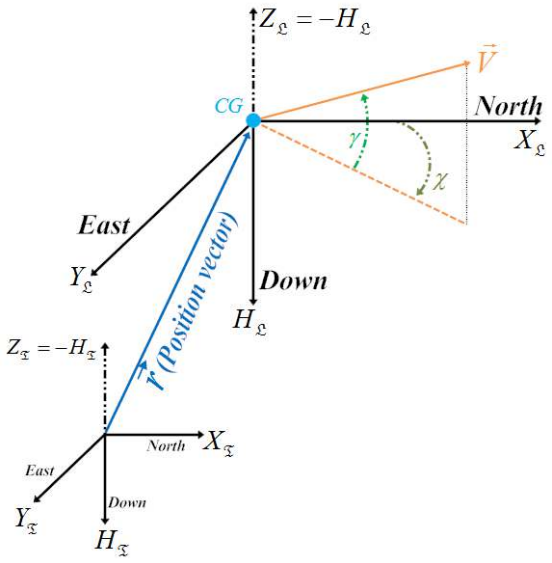

Fig. 2. Coordinate system for Point Mass Model.

In addition from Newton's law, it follows that

$$m\dot{\vec{V}} = \sum \vec{F} \tag{9}$$

where $\vec{F}$ describes the external forces acting on the vehicle, m represents its mass, and $\dot{\vec{V}}$ is the accelerations of the vehicle which are given as

$$\dot{\vec{V}} = \begin{bmatrix} a_{long} \\ a_{lat} \\ a_{vert} \end{bmatrix} = \begin{bmatrix} \dot{V} \\ V\dot{\psi}\cos\theta \\ V\dot{\theta} \end{bmatrix} \tag{10}$$

where a_{long}, a_{lat}, and a_{vert} denotes longitudinal, lateral and vertical accelerations, respectively. Notice that θ, ψ, and V define the attitude of the vehicle. Consequently and without loss of generality, $\dot{\theta}$, $\dot{\psi}$, and $\dot{V}$ can be considered as virtual control inputs. Then,

$$\dot{\theta} = u_1 \tag{11a}$$
$$\dot{\psi} = u_2 \tag{11b}$$
$$\dot{V} = u_3 \tag{11c}$$

In order to incorporate the performance and structural limitations of a real quad-rotor, appropriate constraints are included in the model. These restrictions take the form of bounds on control and some states variables, as follows

$$|u_1| \leq U_{1max} \tag{12a}$$
$$|u_2| \leq U_{2max} \tag{12b}$$
$$|u_3| \leq U_{3max} \tag{12c}$$
$$|\theta| \leq \theta_{max} \tag{12d}$$
$$|V| \leq V_{max} \tag{12e}$$

For more details see [15] - [18].

III. Time Optimal Trajectory Generation

A. Problem statement

We now consider the problem of optimal control in which the objective is to steer the rotorcraft from the actual configuration q_i to the next one q_{i+1} (Eq. 3) in minimum time.

The state and control variables are defined as

$$X(t) = \begin{bmatrix} x(t) & y(t) & z(t) & \theta(t) & \psi(t) & V(t) \end{bmatrix}^T \in \mathbb{R}^6 \tag{13}$$

$$U(t) = \begin{bmatrix} u_1(t) \\ u_2(t) \\ u_3(t) \end{bmatrix} = \begin{bmatrix} \dot{\theta}(t) \\ \dot{\psi}(t) \\ \dot{V}(t) \end{bmatrix} \in \mathbb{R}^3 \tag{14}$$

The vehicle kinematic equations of motion are described by a system of nonlinear differential equations given in equations (8) and (11), which can be expressed as

$$\dot{X}(t) = f\left(X(t), U(t), t\right); \quad \begin{matrix} X(t) \in \mathbb{R}^6 \\ U(t) \in \mathbb{R}^3 \end{matrix} \tag{15}$$

Thus, the time optimal control problem lies in finding an admissible control input $U(t) : [t_0, t_f] \longmapsto \Omega \in \mathbb{R}^3$ such that the system (15) is transferred from an initial configuration

$$X(t_0) = \begin{bmatrix} x_0 & y_0 & z_0 & \theta_0 & \psi_0 & V_0 \end{bmatrix}^T \tag{16}$$

to a final one

$$X(t_f) = \begin{bmatrix} x_f & y_f & z_f & \theta_f & \psi_f & V_f \end{bmatrix}^T \tag{17}$$

with satisfying the constraints imposed on state and control variables (Eq. 12) over some interval time $t \in [t_0 \longrightarrow t_f]$, and minimizing a cost functional

$$J = \min \int_{t_0}^{t_f} dt \tag{18}$$

A theoretical analysis of this problem can be found in [14].

B. Numerical Solution

The basic approach for solving the optimal control problem described above is to transform it into a sequence of nonlinear constrained optimization problems by discretizing the control and/or state variables. This technique is known as Direct Collocation Approach [19]. In this paper, we employ a Nonlinear Programming solver using MATLAB® with respect to the discretized control. The corresponding discretized state variables are determined recursively using a numerical integration scheme (e.g. Euler, Runge-Kutta, etc.) [20].

Therefore, the time interval $[t_0, t_f]$ is divided into N nodes as follows

$$t_0 = \tau_1 \leq \tau_2 \leq t_3 \leq \cdots \leq \tau_N = t_f \tag{19}$$

such that,

$$\tau_k = t_0 + (k-1)\cdot h; \quad h := \frac{t_f - t_0}{N-1}, k = 1, \ldots, N \tag{20}$$

Thus, the vector of unknown variables is composed of the control inputs over all nodes and the final time t_f as it is shown below

$$\xi = \left[t_f, U_1^T, U_2^T, \ldots, U_N^T\right] \in \mathbb{R}^{N_\xi}; \quad N_\xi = 3N + 1 \quad (21)$$

and the state variables are computed recursively using Euler approximation applied to the differential equations (15) which yields to the following

$$X_{k+1} = X_k + h \cdot f\left(X_k, U_k\right); \quad k = 1, \ldots, N-1 \quad (22)$$

with the initial and final conditions given in (16) and (17).

From the previous discussion, the problem of optimal control can be described as following

$$\begin{aligned}
&\text{Minimize} && J = t_f && \text{(23a)}\\
&\text{Subject to} && \dot{X_k} = f\left(X_k, U_k\right) && \text{(23b)}\\
& && X(t_1) = X_0 && \text{(23c)}\\
& && X(t_N) = X_f && \text{(23d)}\\
& && C_{lw} \leq U_k \leq C_{up} && \text{(23e)}\\
& && S_{lw} \leq S\left(X_k\right) \leq S_{up} && \text{(23f)}
\end{aligned}$$

where $k = 1, 2, \ldots, N$, C_{lw} and C_{up} are lower and upper bounds on control inputs across all nodes. The k^{th} set of control rate limits, expressed in equation (23e), is given as

$$\begin{bmatrix} \dot{\theta}_{min} \\ \dot{\psi}_{min} \\ \dot{V}_{min} \end{bmatrix} \leq \begin{bmatrix} \dot{\theta}_k \\ \dot{\psi}_k \\ \dot{V}_k \end{bmatrix} \leq \begin{bmatrix} \dot{\theta}_{max} \\ \dot{\psi}_{max} \\ \dot{V}_{max} \end{bmatrix} \quad (24)$$

Moreover, S_{lw} and S_{up} denote the lower and upper constraints enforced on the path. The k^{th} set of path restrictions, presented in equation (23f), is shown as

$$\begin{bmatrix} \theta_{min} \\ V_{min} \end{bmatrix} \leq \begin{bmatrix} \theta_k \\ V_k \end{bmatrix} \leq \begin{bmatrix} \theta_{max} \\ V_{max} \end{bmatrix} \quad (25)$$

Next section deals with the problem of trajectory tracking for a quadrotor.

IV. Trajectory Tracking Problem

Once a feasible and flyable reference trajectory is generated, it is important to examine its applicability and compatibility with the dynamics of the quadrator. For this purpose, we employ the trajectory generated by the previous method to the rotorcraft's rigid body model (Eq. 2) as reference signals ; and we design an autopilot to ensure the trajectory tracking. The control strategy used in these paper is based on the control laws introduced in [12] and [13] for stabilizing quadrotor at hover.

The controller regulates each one of the state variables in a sequence according to a predefined priority rule as follows : First of all, the desired altitude (z) is reached using the control input u. Then, the yaw angle (ψ) is controlled through τ_ψ. Next, the desired values of pitch angle (ϕ) and y-displacement are reached by controlling τ_ϕ. Finally, the control input τ_θ is used to obtain the desired pitch angle (θ) and x-displacement values.

Next, the following definition is fundamental for the control strategy.

***Definition** 1:* The function $\sigma\left(t\right)$ is said to be a saturation function if and only if

$$\left|\sigma\left(t\right)\right| \leq M; \forall M \in \mathbb{R}^+ \quad (26)$$

A. Altitude and Yaw Control

The control of z-displacement is ensured through the following control input

$$u = \sec(\theta)\sec(\phi)\bar{r} \quad (27)$$

where

$$\bar{r} = -\mathfrak{K}_{z1}\left(\dot{z} - \dot{z}_{ref}\right) - \mathfrak{K}_{z2}\left(z - z_{ref}\right) + mg \quad (28)$$

with, $\mathfrak{K}_{z1}$ and $\mathfrak{K}_{z2}$ are positive constant, $\dot{z}_{ref}$ and z_{ref} are the desired vertical velocity and altitude respectively. In addition, θ and ϕ are assumed to be limited such that they can not reach 90 degrees.

On the other side, the yaw angle is controlled by applying

$$\tau_\psi = -\sigma_{\psi 1}\left(\mathfrak{K}_{\psi 1}\left(\dot{\psi} - \dot{\psi}_{ref}\right)\right) - \sigma_{\psi 2}\left(\mathfrak{K}_{\psi 2}\left(\psi - \psi_{ref}\right)\right) \quad (29)$$

Substituting equations (28) and (29) into (2c) and (2d), it follows that : $\dot{z} \mapsto \dot{z}_{ref}$, $z \mapsto z_{ref}$, $\dot{\psi} \mapsto \dot{\psi}_{ref}$ and $\psi \mapsto \psi_{ref}$.

B. Roll and Lateral Position Control

Once $\dot{z}$ and z are stabilized, the equations (2a) and (2b) can be reduced to

$$\ddot{x} = -g\tan(\theta)\sec(\phi) \quad (30a)$$

$$\ddot{y} = g\tan\left(\phi\right) \quad (30b)$$

Considering the subsystem (ϕ, y) given by equations (30b) and (2f). Then, the control input for this subsystem is given by

$$\begin{aligned}
\tau_\phi = \quad & -\sigma_{\phi 1}\left(\mathfrak{K}_{\phi 1}\left(\dot{y} - \dot{y}_{ref}\right)\right) - \sigma_{\phi 2}\left(\mathfrak{K}_{\phi 2}\left(y - y_{ref}\right)\right)\\
& -\sigma_{\phi 3}\left(\mathfrak{K}_{\phi 3}\left(\dot{\phi}\right)\right) - \sigma_{\phi 4}\left(\mathfrak{K}_{\phi 4}\left(\phi - \phi_{ref}\right)\right)
\end{aligned} \quad (31)$$

where the controller gain parameters $\mathfrak{K}_{\phi 1}$, $\mathfrak{K}_{\phi 2}$, $\mathfrak{K}_{\phi 3}$ and $\mathfrak{K}_{\phi 4}$ are positive constant.

C. Pitch and Forward Position Control

From equations (31) and (30b) it follows that $\phi \mapsto 0$. Then, the equation (30a) becomes $\ddot{x} = -g\tan(\theta)$ Finally, the subsystem (θ, x) is controlled through τ_θ which is given by

$$\begin{aligned}
\tau_\theta = \quad & \sigma_{\theta 1}\left(\mathfrak{K}_{\theta 1}\left(\dot{x} - \dot{x}_{ref}\right)\right) + \sigma_{\theta 2}\left(\mathfrak{K}_{\theta 2}\left(x - x_{ref}\right)\right)\\
& -\sigma_{\theta 3}\left(\mathfrak{K}_{\theta 3}\left(\dot{\theta}\right)\right) - \sigma_{\theta 4}\left(\mathfrak{K}_{\theta 4}\left(\theta - \theta_{ref}\right)\right)
\end{aligned} \quad (32)$$

where the controller gain parameters $\mathfrak{K}_{\theta 1}$, $\mathfrak{K}_{\theta 2}$, $\mathfrak{K}_{\theta 3}$ and $\mathfrak{K}_{\theta 4}$ are positive constant.

V. Simulation Results

In this section, two different scenarios are considered. Each one consists of an initial configuration, a final one, and several way-configurations. For both cases, the trajectory is divided into several segments depending on the number of way-configurations to visit. Then, the optimization process described in sec. III-B is applied for every segment separately. Once the reference trajectory is generated, an autopilot is designed to evaluate the validity of a such trajectory.

The constraints on pitch angle, velocity, and control variables are provided in Table I.

TABLE I

Restrictions on state and control variables

Minimum	Variable	Maximum	Units
- 15	θ	15	deg
0.001	V	0.2	m/sec
- 5	$\dot{\theta}$	5	deg/sec
- 10	$\dot{\psi}$	10	deg/sec
- 0.01	$\dot{V}$	0.01	m/sec^2

A. Trajectories at fixed altitude (2D)

The objective in this case is to generate a reference trajectory assuming that the vehicle is moving only in the horizontal plane ($x \times y$). Which means that both $\dot{\theta}$ and θ are equal to zero. Then, the equations of motion presented in equations (8) and (11) are reduced to the following

$$\begin{aligned} \dot{x} &= V\cos\psi \\ \dot{y} &= V\sin\psi \\ \dot{\psi} &= u_1 \\ \dot{V} &= u_2 \end{aligned}$$

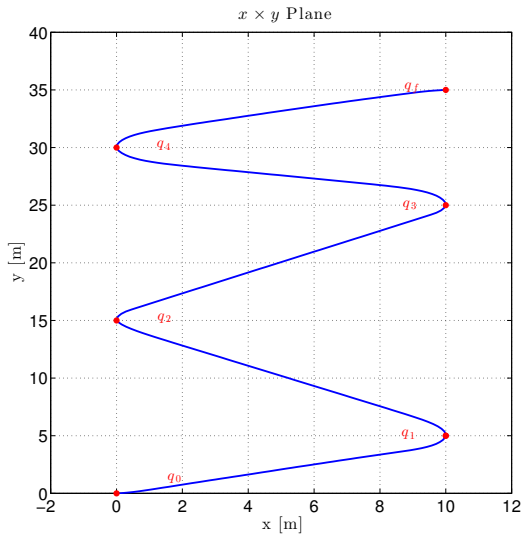

Fig. 3. Flying at a constant altitude trajectory.

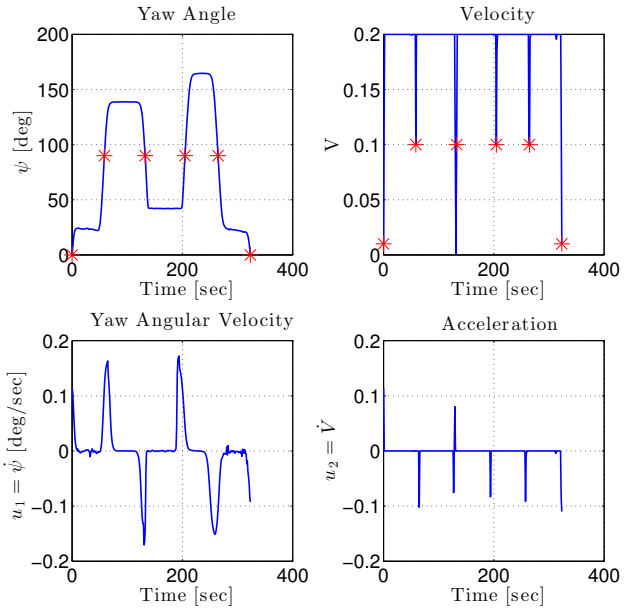

Fig. 4. Time profile of yaw angle ψ, vehicle's velocity and their rate of change $\dot{\psi}$, $\dot{V}$ respectively

The number of nodes (N) used in each segment is 84, and the interior point algorithm included in *fmincon solver* in MATLAB® is used to compute optimal trajectory. The initial configuration q_0, the final one q_f, and the way-configurations q_i, in this case, are presented in Table II. The position, orientation, velocity, and control inputs of the aerial vehicle are illustrated in Figures 3 and 4.

TABLE II

Configurations to be visited during the traveled trajectory

	x $[m]$	y $[m]$	ψ $[deg]$	V $[m/sec]$
q_0	0	0	0	0.01
q_1	10	5	90	0.1
q_2	0	15	90	0.1
q_3	10	25	90	0.1
q_4	0	30	90	0.1
q_f	10	35	0	0.01

Notice the final configuration is reached in $t_f = 323.2$ [sec].

B. Trajectories in 3D space

In this case, the quad-rotor is assumed to fly around a structure for the purpose of construction inspection. Each segment is descretized over 70 nodes, and, as in the previous case, the interior point algorithm included in *fmincon solver* in MATLAB® is used to generate the minimal time trajectory. The initial configuration q_0, the final one q_f, and the tenth way-configurations q_i ; $i = 1, \ldots, 10$ are presented in Table III. While, the position, orientation, velocity, and control inputs of the vehicle are illustrated in Figures 5- 7.

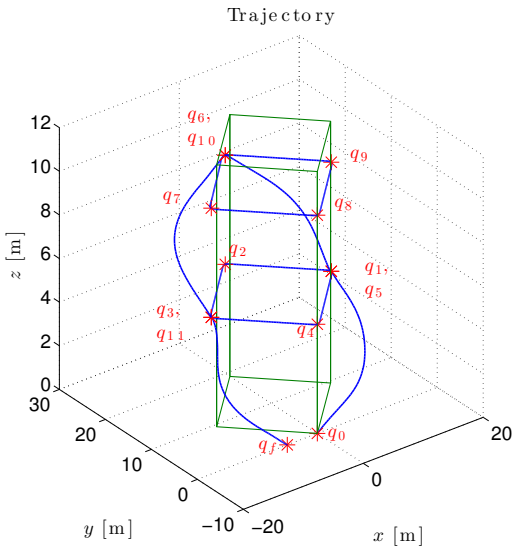

Fig. 5. 3D view of structure inspection scenario.

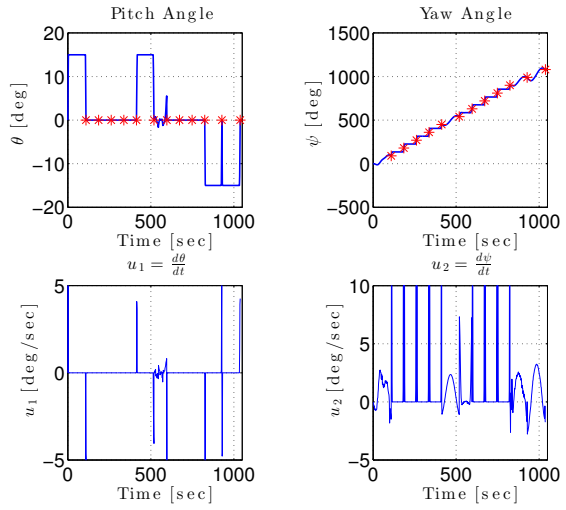

Fig. 6. Time profile of pitch θ, yaw ψ and their rate of change $\dot{\theta}$, $\dot{\psi}$ respectively.

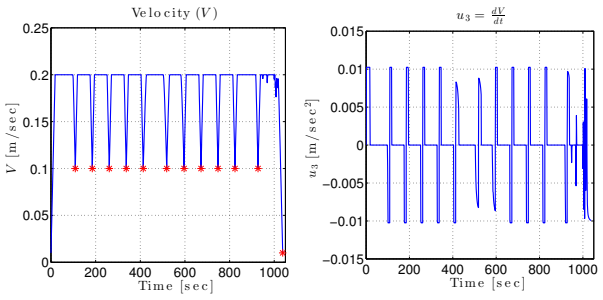

Fig. 7. Time profile of vehicle's velocity V and $\dot{V}$ acceleration.

Notice that the required time to complete the trajectory is $t_f = 1038\ [sec] = 17.3\ [min]$.

TABLE III
CONFIGURATIONS TO BE VISITED DURING THE TRAVELED TRAJECTORY.

	$x\ [m]$	$y\ [m]$	$z\ [m]$	$\theta\ [deg]$	$\psi\ [deg]$	$V\ [m/sec]$
q_0	0	0	0	0	0	0.01
q_1	10	10	5	0	90	1
q_2	0	20	5	0	180	1
q_3	-10	10	5	0	270	1
q_4	0	0	5	0	360	1
q_5	10	10	5	0	450	1
q_6	0	20	10	0	540	1
q_7	-10	10	10	0	630	1
q_8	0	0	10	0	720	1
q_9	10	10	10	0	810	1
q_{10}	20	10	10	0	900	1
q_{11}	-10	10	5	0	990	1
q_f	-5	0	0	0	1080	0.01

Remark that the choice of the number of nodes plays an important role in determining the size of the optimization problem. In this paper, the number of nodes N is chosen in a such way so that the resulting trajectory is smooth and calculation time is still reasonable.

Observe that the previous results can be also obtained using Sequential-Quadratic-Programming (SQP) method included in *fmincon solver* in MATLAB® which is more advantageous in terms of computation time and algorithm convergence.

C. Trajectory Tracking

In this part, we treat the tracking problem in order to evaluate the applicability and the validity of the calculated reference trajectory with the dynamics of quadrotor. For this end, we take the results found in the section V-A as references for the full dynamic quadrotor model presented in equation (2). The control parameters and the limitations of saturation functions values were chosen to ensure a stable well-damped response specially for x, y and ψ variables.

The performance of the designed autopilot is illustrated in the Figures 8 - 12. In these figures, the solid line represents the system response and the dashed line describes the desired value or trajectory. The time profile of the yaw angle and its derivative are shown in Figure 8. While, the time profile of the x and y displacement and their absolute error are presented in Figures 9 and 10 respectively. In Figure 11, the time profile of pitch and roll angles are depicted, and the control inputs are described in Figure 12.

Note that the controller has a good performance to tracks the yaw angle, x and y displacements. While, it has not the same efficiency to follow the yaw angular velocity. This behavior is due to the fact that the gain assigned to yaw angle (i.e. $\mathfrak{K}_{\phi 2}$) is more important than the one dedicated to its derivative (i.e. $\mathfrak{K}_{\phi 1}$). On the other hand, observe that the desired pitch and roll angles are set to be zeros but the real θ and ϕ differs for some periods of time which is due to movements on x and y axis and acceleration/deceleration effects.

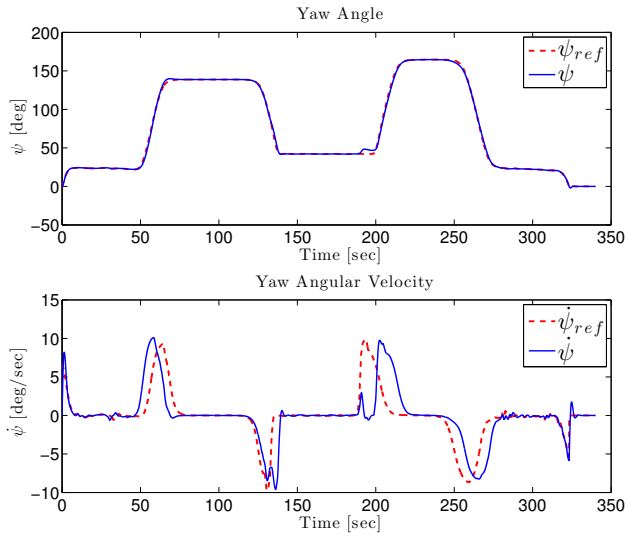

Fig. 8. Yaw angle of quadrotor.

VI. Conclusion

The problem of reference trajectory generation for an autonomous quadrotor flying vehicle is studied in this paper. In addition, an autopilot has been designed to validate a predefined trajectory. The vehicle is modeled in two different ways. A point mass model dedicated for the computation of the reference trajectory, and a rigid body model devoted to tracking problem. We formulated a minimum time optimal control problem to generate the reference trajectory. This formulation is converted to nonlinear constrained optimization problems and is solved by a direct collocation approach. Some simulations were realized and some graphs were presented to validate the trajectory generation method

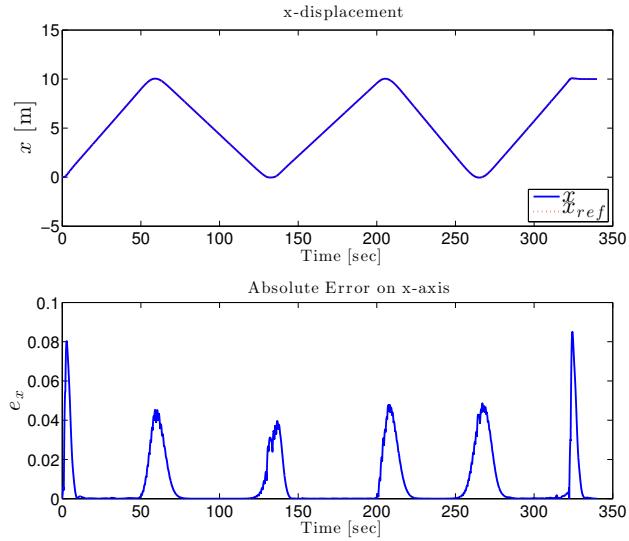

Fig. 9. x-displacement of quadrotor.

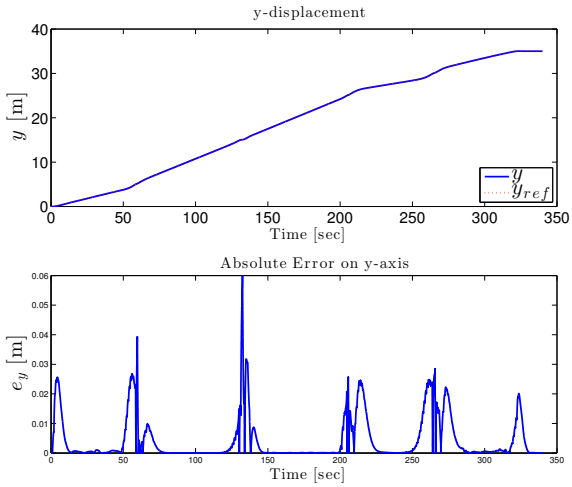

Fig. 10. y-displacement of quadrotor.

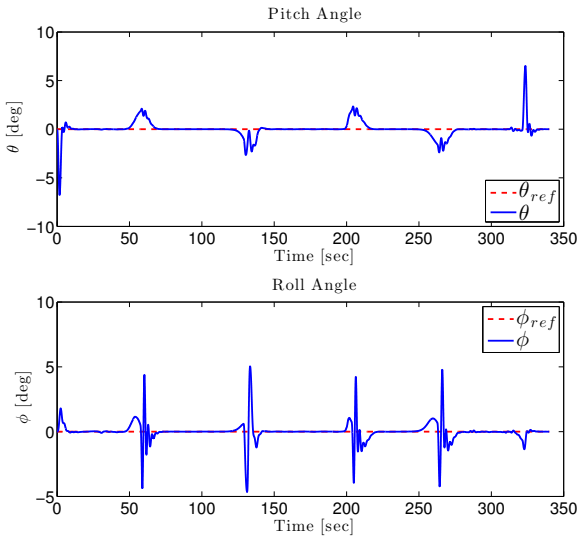

Fig. 11. Time profile of pitch (θ) and roll (ϕ) angles.

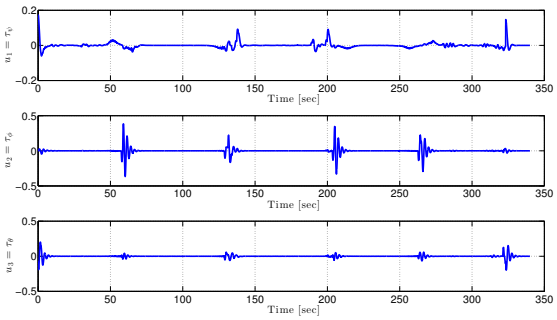

Fig. 12. Control inputs : τ_ψ, τ_ϕ and τ_θ.

and to show its applicability and compatibility with the full

dynamics quadrotor model.

REFERENCES

[1] Wilson J.R., "UAV Roundup 2011", Aerospace America, Volume 49, No. 3., pp. 22-31, March 2011.

[2] Dubins L. E., "On Curves of minimal length with a constraint on average curvature, and with prescribed initial and terminal positions and tangents", American Journal of Mathematics, Volume 79, pp. 497-516, 1957.

[3] Yang G., and Kapila V., "Optimal Path Planning for Unmanned Air Vehicle with Kinematic and Tactical Constraints", In Proceedings of the 41st IEEE Conference on Decision and Control, Las Vegas, NV, 2002.

[4] Wong H., Kapila V., and Vaidyanathan R., "UAV optimal path planning using C-C-C class paths for target tourning", In Proceedings of the 43rd IEEE Conference on Decision and Control, Bahamas, 2004.

[5] Ambrosino G., Ariola M., Ciniglio U., Corraro, De Lellis E., and Pironti A., "Path Generation and Tracking in 3-D for UAVs", IEEE Transactions on Control Systems Technology, Volume 17, No. 4, pp. 980-988, July 2009.

[6] Anderson E. P., Beard R. W., and McLain T. W., "Real-Time Dynamic Trajectory Smoothing for Unmanned Air Vehicles", IEEE Transactions on Control System Technology, Volume 13, No. 3, pp. 471-477, May 2005.

[7] Boukraa D., Bestaoui Y., and Azouz N., "Three Dimensional Trajectory Generation for an Autonomous Plane", International Review of Aerospace Engineering, Volume 1, No. 4, August 2008.

[8] Judd K. B., and McLain T. W., "Spline Based Path Planning for Unmanned Air Vehicles", AIAA Guidance, Navigation and Control Conference and Exhibit, Montreal, CANADA, August 2001.

[9] Vázques G. B., Sossa A. J. H., and Díaz-de-León S. J. L., "Auto Guided Vehicle Control Using Expanded Time B-Splines", IEEE International Conference on Systems, Man, and Cybernetics, San Antonio, TX, October 1994.

[10] Berglund T., Jonsson H., and Söderkvist I., "An Obstacle Avioding Minimum Variation B-Spline Problem", In Proceedings of International Conference on Geometric Modeling and Graphics, London, UK, July 2003.

[11] Dyllong E., and Visioli A., "Planning and Real-Time Modifications of a Trajectory Using Spline Techniques", Robotica, Volume 21, pp. 475-482, 2003.

[12] Castillo P., Lozano R., and Dzul A., "Stabilization of a Mini Rotorcraft with Four Rotors", IEEE Control Systems Magazine, December 2005.

[13] Castillo P., Lozano R., and Dzul A. E., "Modelling and Control of Mini-Flying Machines", Springer, 2005.

[14] Bestaoui Y., and Kahale E. "Time Optimal Trajectories of a Lighter-Than-Air Robot in a Steady Wind", Journal Of Aerospace Information Systems Volume 10, Number 4, pp. 155-171, 2013.

[15] Hull D. G., "Fundamentals of Airplane Flight Mechanics", Springer, 2007.

[16] Kahale E., Castillo P., and Bestaoui Y., "Autonomous Path Tracking of a Kinematic Airship in Presence of Unknown Gust", Journal of Intelligent and Robotic Systems, Volume 69, Issue 1-4 , pp 431-446, January 2013.

[17] Imado F., Heike Y., and Kinoshita T., "Research on a New Aircraft Point Mass-Model", Journal of Aircraft, Volume 48, Number 4, pp 1121 - 1130, July - August 2011.

[18] Stevens B. L., and Lewis F. L., "Aircraft Control and Simulation, 2nd Edition", John Wiley & Sons Inc., 2003.

[19] Subchan S., Zbikowski R., "Computational Optimal Control Tools and Practice", John Wiley & Sons Inc., 2009.

[20] Büskens C., and Maurer H., " SQP-methods for solving optimal control problems with control and state constraints : Adjoint variables, sensitivity analysis and real-time control", Journal of Computational and Applied Mathematics, Volume 120, Issues 1-2, pp. 85-108, August 2000.